



Roles of Packed Bed Porosity on Performance of Biofilter Microbial Fuel Cell in Synthetic Landfill Leachate Treatment

Songyot Mongkulphit¹, Supawadee Siripratum¹, Warista Chumroen¹, and Petch Pengchai^{2,*}

ARTICLE INFO

Article history:

Received: 18 January 2020

Revised: 19 September 2020

Accepted: 7 December 2020

Keywords:

Microbial fuel cell

Media bed porosity

Shears stress

Landfill leachate

Biofilter

Biomass

ABSTRACT

Microbial fuel cell (MFC) technology has been attracted to research attention as a preferable option to harvest apparently pollution-free energy from wastewater treatment. In this study, 4 biofilter-microbial fuel cells (BMFCs) were built up and applied to synthetic landfill leachate. The effect of media bed porosity in the range of 0.75 to 1 on BMFCs performance was taken into account. It was found that a BMFC with 0.75 bed porosity had the highest performance with chemical oxygen demand (COD) removal rate of 3565.2 mgL-1hr-1 and maximum electrical power of 44×10^{-6} W. Lower bed porosity has been proved to provide higher shear stress, greater biomass, higher removal efficiency, and higher maximum electrical power with remarkable regression coefficients from 0.92 to 0.98. It can be said that media bed porosity plays an important role as the shear stress and biomass controller in BMFC performance.

1. INTRODUCTION

MFC technology has gained much attention due to its ability to produce electricity from wastewater treatment via microorganisms. Different configurations of MFCs have been studied, such as single-chambers, dual-chamber MFCs [1], different electrode materials, membrane vs. membrane-less MFCs [2], MFCs with and without the addition of mediators [3]. However, membrane-less-tubular MFC without the addition of mediators is of our interest due to its economic advantage and wastewater treatment capacity in scaled-up MFC [4]. In terms of substrate, we focus on landfill leachate as the highest open circuit voltage (OCV = 1.29 V) ever reported in the MFC system was observed in landfill leachate fed MFCs [5]. In our previous study, 7.8 L of membrane-less-BMFCs were built up adapting the MFC configuration of Sukkasem et al. [6]. One of them showed high removal of biological oxygen demand (99%) in real landfill leachate with very low maximum power generation of 4×10^{-6} W (4×10^{-3} W m⁻²). In this study, our BMFCs were reconstructed with changes in volume, material, and electrode positions to enhance the energy production process. Among many power generations limiting factors, a number of microbes attached on the surface of anode were recognized as the primary element which drives the electro genesis process [7]. Therefore, parameters that enriched the electroactive biofilm in an anode chamber are the matter of our interest.

When liquid flows through the filter media in an anode chamber of BMFC, hydrodynamic shear force resulted from surface friction and kinetic energy losses can be calculated using media bed porosity (ϵ) as an input parameter [8]. Li et al. [7] reported that this shear force changed the structure of the biofilm, and consequently affected the MFC current generation. Pham et al. [9] found that enrichment at a shear rate of about 120 s⁻¹ resulted in the production of a current and power output of 2 to 3 times higher than those in the case of low shear rates (around 0.3 s⁻¹). The increasing high shear rates initially resulted in an increase of the total DNA amount of the bacterial cells attached to the electrode but, above the estimated shear rate of 120 s⁻¹, both the current and the DNA amount decreased [9]. According to the aspects described above, τ which can be calculated as a function of ϵ could affect the biomass attached to the packed bed and result in change of the power generation. Consequently, appropriate ϵ should be applied to BMFCs, so as to cause suitable τ and high-power output.

However, for membrane-less-tubular MFCs with media packed bed, an effect of ϵ on MFCs performance is not widely publicized. Therefore, in this study, we constructed BMFCs with various ϵ and fed them with synthetic landfill leachate. Shear stress and biomass associated with each ϵ condition was determined and analyzed for their relationship with ϵ values.

¹Faculty of Engineering, Maharakham University, Thailand.

²Circular Resources and Environmental Protection Technology Research Unit: CREPT, Environmental Engineering Laboratory, Faculty of Engineering, Maharakham University, Maharakham, 44150, Thailand..

*Corresponding author: P. Pengchai; Phone: +66-1-881-1860; Fax: +66-43-754-316; Email: petch.p@msu.ac.th.

2. METHODOLOGY

2.1 BMFC construction

Four membrane-less BMFCs were constructed using polyvinyl chloride pipes as shown in Fig. 1. Anode chambers with diameter of 10 cm and height of 50 cm (see Fig. 2) were filled with filter media made from bunches of 20 nylon fibers (diameter of 1.0 mm and length of 10 cm) as shown in Fig. 3. a), Media bed porosities of 4 BMFCs were calculated from $\varepsilon = V_v/V_t$, where V_v was volume of voids (L) and V_t was total media bed volume (L). By varying numbers of nylon branches, ε of each BMFC was arranged, i.e., 0-bunch-filter media for $\varepsilon = 1$, 142-bunch-filter media for $\varepsilon = 0.95$, 425-bunch-filter media for $\varepsilon = 0.85$, and 710 bunch-filter media for $\varepsilon = 0.75$. Triangle graphite plate with projected surface area of 41.6 cm^2 (6.90-cm width, 6.02-cm height, 1.5-cm thickness) was placed in the middle of each anode chamber as an anode. Ellipse graphite plate (see Fig. 3. b)) with projected surface area of 665.2 cm^2 (6.62-cm width, 4.0-cm height, 1.5-cm thickness) was placed on the top of each BMFC as an air-cathode. The distance between the cathode and anode of each BMFC was 51 cm.



Fig. 1. Four membrane-less, single chamber BMFCs used in this study.

2.2 Synthetic landfill leachate

Synthetic landfill leachate used in this study was modified from Halim's experiment [10] by dissolving the following components in water (amount per liter): 7 mL of acetic acid (CH_3COOH), 5 mL of propionic acid ($\text{C}_3\text{H}_6\text{O}_2$), 0.156 g of MgSO_4 , 2.882 g of CaCl_2 , 0.324 g of Na_2CO_3 , 2.4g of $(\text{COO}\cdot\text{NH}_4)_2\cdot\text{H}_2\text{O}$, 1.44g of NaCl , and 1 mL of trans metals solution (TMS). NaOH solution was added to the synthetic landfill leachate for pH 7 adjustment. The compositions of TMS was (amount per liter) CuCl_2 , 0.04g; $(\text{NH}_4)_2\text{SO}_4\cdot\text{NiSO}_4\cdot 6\text{H}_2\text{O}$, 0.50 g; $(\text{NH}_4)_2\text{Fe}(\text{SO}_4)_2\cdot 6\text{H}_2\text{O}$, 2

g; $\text{BaCl}_2\cdot 2\text{H}_2\text{O}$ 0.05 g; $\text{MnSO}_4\cdot 4\text{H}_2\text{O}$ 0.5 g; 96% sulfuric acid (H_2SO_4) 1 mL [10]. Influent synthetic landfill leachate at the end of the treatment period contained 17.778 g L^{-1} of COD; 2.92 g L^{-1} of BOD; 0.0025 g L^{-1} of ammonia; 0.0068 g L^{-1} of nitrate; and 0.0128 g L^{-1} of sulfate.

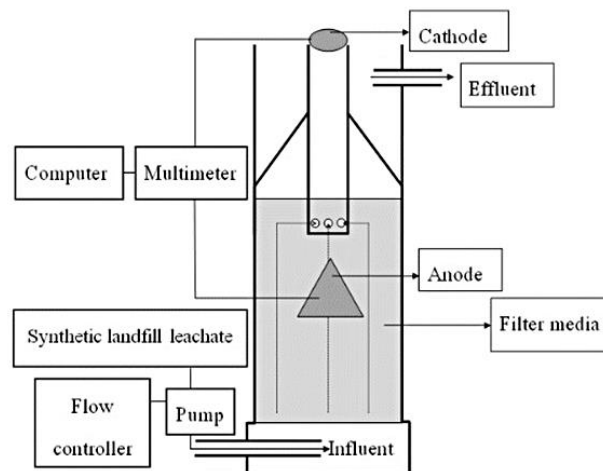


Fig. 2. Reactor design.



Fig. 3. a) Filter media, b) the position of a cathode.

2.3 Start-up

Start-up operation included 2 phases. As existing microorganism enrichment phase, synthetic landfill leachate was kept in each BMFC for 26 days before 120 L of new synthetic landfill leachate was fed into the BMFCs with 100% recirculation ratio for 5 days. A microorganism which in the flavor of synthetic landfill leachate should be enriched and attached to the media during this phase. However, since the OCV measured in this phase was lower than 0.2 V, the addition of microorganism from outer source is needed. Consequently, photosynthetic bacteria (PB) seeding phase was performed by adding 5 L of PB mixture (prepared from Siam Rhodo PB liquid fertilizer) to 120 L of synthetic landfill leachate. The mixture was fed to BMFCs with 100% recirculation ratio for 5 days.

2.4 Treatment of landfill leachate by BMFCs

Synthetic landfill leachate was continuously fed to each BMFC with a flow rate of 40 L day^{-1} . Hydraulic retention times (HRTs) were 3.52 hours for BMFC with $\varepsilon = 1$; 3.36

hours for $\varepsilon = 0.95$; 2.98 hours for $\varepsilon = 0.85$; and 2.80 hours for $\varepsilon = 0.75$. Basic conditions inside anode chambers were measured along the experiment using DO meter for dissolved oxygen (DO), ORP meter for oxidation reduction potential (ORP), and pH meter for pH measurements. Compositions of the influent and effluent were analyzed during the 7-day process using closed-reflux titrimetric method for COD, Nessler's method for total ammonia nitrogen (TAN-N), spectrophotometer method for nitrate nitrogen (NO_3^- -N), turbidimetric method by spectrophotometer for sulfate (SO_4^{2-}), evaporation method for total solid (TS) analysis, and gravimetric analysis method for total dissolved solid (TDS) analysis. Real-time monitoring of OCV was done for each BMFC throughout the experiment using a bench multimeter (GDM-8255A, Good Will Instrument Co., Ltd.).

2.5 Polarization experiment

At the end of the treatment operation, polarization experiment was done for each BMFC by connecting anode to the cathode through 8 various external resistances, i.e., 10,000; 5,000; 2,500; 2,000; 1,250; 1,000; 800, and 100 Ohms. Voltages (V) across each external resistance (R_{ext}) were measured and applied to Eq. 1 [11] to calculate an electrical power (P) transferred to the R_{ext} , whereas I is the electrical current.

$$P = VI = I^2 R_{\text{ext}} \quad (1)$$

The maximum value (P_{max}) for each BMFC was determined and used to represent an electrical performance of the cell. Internal resistance (R_{int}) at P_{max} , another important aspect for MFC practical application, was estimated based on Eqs. 2-4 modified from Kamau et al. [11]. E_{emf} is electromotive force (V) of BMFC.

$$E_{\text{emf}} = IR_{\text{ext}} + IR_{\text{int}} \quad (2)$$

$$I = E_{\text{emf}} / (R_{\text{ext}} + R_{\text{int}}) \quad (3)$$

$$P = (E_{\text{emf}} (R_{\text{ext}} + R_{\text{int}}))^2 R_{\text{ext}} = E_{\text{emf}}^2 / (R_{\text{ext}} + 2R_{\text{int}} + (R_{\text{int}}^2 / R_{\text{ext}})) \quad (4)$$

When P becomes P_{max} , the denominator in Eq. 4 should become minimum [11]. Therefore, Eq. 5 which shows the differentiating of the denominator with respect to R_{ext} should become zero [11]. Consequently, the R_{int} at P_{max} condition is considered to be equal to the R_{ext} due to Eq. 6.

$$d(R_{\text{ext}} + 2R_{\text{int}} + (R_{\text{int}}^2 / R_{\text{ext}})) / dR_{\text{ext}} = 1 - (R_{\text{int}}^2 / R_{\text{ext}}^2) \quad (5)$$

$$R_{\text{int}}^2 / R_{\text{ext}}^2 = 1 \quad (6)$$

2.6 Hydrodynamic shear stress estimation

Hydrodynamic shear stress (τ , dyn/cm²) in an anode chamber of each BMFC was calculated using Eqs.7-8 whereas ν is viscosity (103 gm⁻¹·s⁻¹); ρ is liquid density (103 gm⁻³); F is the flow rate (m³·s⁻¹); S is a section area

(m²); D_p is the diameter of randomly packed particles (m); V_p is the volume of filling non-spherical particles (m³) and A_p is the surface of filling non-spherical particles (m²) [8].

$$\tau = (25\nu F(1-\varepsilon) / D_p S \varepsilon^2) + (1.75\rho F^2 / S^2 \varepsilon^2) \quad (7)$$

$$D_p = 6V_p / A_p \quad (8)$$

With various ε values as the main independent variable, different values were calculated as the dependent variable by substituting Eq.7 and Eq.8 with $\nu = 1.005 \text{ g m}^{-1}\cdot\text{s}^{-1}$; $=1.014363 \text{ g m}^{-3}$; $F = 4.629 \times 10^{-7} \text{ m}^3\text{s}^{-1}$; $S = 0.00785 \text{ m}^2$; $V_p = 1.014 \times 10^{-6} \text{ m}^3/\text{bunch}$; $A_p = 622.914 \times 10^{-6} \text{ m}^2/\text{bunch}$.

2.7 Biomass measurement

At the end of the operation, the biomass attached to the filter media (m_b) was determined. Ten bunches of filter media were randomly sampled up from each BMFC and put into a glass bottle filled with 300 mL distilled water. The glass bottles were shaken in an ultrasonic sonicator bath (53 kHz, 25 °C, LHC series 35/53 kHz Dual Frequency Ultrasonic Cleaner, Shanghai Kudos Ultrasonic Instrument Co., Ltd.) for 2 hours before their inside liquids were taken to TS measurement. Measured TS value was divided by 10 to estimate the biomass attached to 1 bunch of filter media (m_1). Thus, total biomass attached to the filter media of each BMFC (m_b) was calculated by multiplying m_1 to the number of bunches of filter media filled in each anode chamber.

3. RESULTS AND DISCUSSION

3.1 Start-up period

Synthetic landfill leachate with 18.701 gL⁻¹ of COD; 0.00967g L⁻¹ of TAN-N; and 0.00655g L⁻¹ of NO_3^- -N at the first day of recirculation period of existing microorganism enrichment phase became less polluted at the last day of PB seeding phase with 2.927 to 5.926 g L⁻¹ of COD; 0.0038 to 0.0061 g L⁻¹ of TAN-N; and 0.0030 to 0.0036 gL⁻¹ of NO_3^- -N. Inside all anode chambers, DO, ORP and pH ranged between 0.00054 to 0.0011 gL⁻¹; -333 to -407 mV, and 8.1 to 8.5, respectively. Comparing to low OCVs (-0.004 to 0.039 V) at the enrichment phase, high OCVs (0.16 to 0.72 V) were detected in the PB seeding phase. P_{max} at the end of the start-up period ranged between 14.8-26.4 $\times 10^{-6}$ W. The above results implied the growth of electrogenic microorganisms in each B-MFC and their wastewater treatment ability.

3.2 Landfill leachate treatment

During a treatment period, conditions inside the anode chambers were similar to those in the start-up period with DO of 0.04 to 0.27 mgL⁻¹; ORP of -370 to -404 mV; and pH of 7.46 to 8.34. An effluent at day 7th of the treatment operation contained 5.647 to 11.566 gL⁻¹ of COD; 0.0163 to 0.0174gL⁻¹ of TS; and 0.0162 to 0.0172g L⁻¹ of TDS. Most

of the TS were in the form of TDS. Removal efficiencies and removal rates of COD and TDS appeared in order of lower ϵ values. Highest removal rate of COD ($3.5652 \text{ gL}^{-1}\text{h}^{-1}$, 61.6% efficiency) and TDS ($0.0014 \text{ gL}^{-1}\text{h}^{-1}$, 19.6% efficiency) were observed at $\epsilon = 0.75$ as shown in Fig. 4 As microbial attachable area become larger at $\epsilon = 0.75$, higher microbial metabolism could occur and cause higher removal rate than in the lower ϵ .

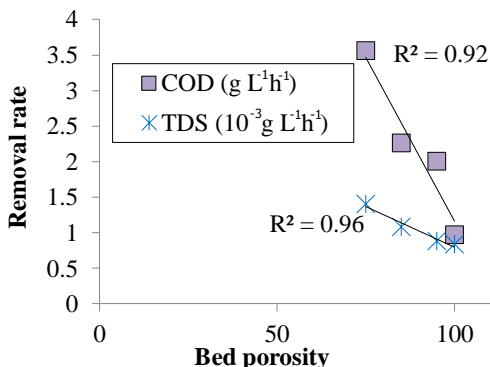


Fig. 4. Removal rates of BMFCs at the last day of synthetic landfill leachate treatment.

3.3 Electricity generation

In the treatment period, the highest OCV in this study was 0.6 V which was higher than OCVs of MFCs with CNT/Pt-coated CP cathode reported in Mashkour et al.'s article [12]. but slightly lower than OCVs of a dual chamber MFC with an addition of 0.2 g L^{-1} hexacyanoferrate in Izadi et al.'s study [13]. In this 0.301 to 0.600 V while the others were in ranges of 0.314 to 0.392 V for $\epsilon = 1$, 0.227 to 0.423 V for $\epsilon = 0.95$, and 0.215 to 0.357 V for $\epsilon = 0.85$. Results of polarization experiment at the last day of the treatment period were shown in Fig. 5. P_{max} values were higher for the lower ϵ condition and BMFC achieved the highest OCV and P_{max} ($43.96 \times 10^{-6} \text{ W}$ or $10.57 \times 10^{-3} \text{ Wm}^{-2}$) at the lowest ϵ value (0.75). Comparing to $9.78 \times 10^{-3} \text{ Wm}^{-2}$ P_{max} of mediator-less MFC in Izadi et al.'s study [13], comparable electricity generation was achieved by using our low-cost BMFC configuration. Interestingly, R_{int} during P_{max} generation of all BMFCs were equal (2,500 ohm) despite of different ϵ conditions. Consequently, the difference of P_{max} values among 4 BMFCs was not caused by the change in R_{int} value. From definition that voltage losses can be dissected into activation loss, ohmic loss, and concentration loss which existed in 3 regions of the polarization graph [14], the concentration loss seemed to have large effect on BMFCs in this study. In Fig. 5, P_{max} of every BMFC dropped rapidly due to the drop of voltages in the concentration loss region. Especially in case of $\epsilon = 0.75$, P_{max} might have been larger than $43.96 \times 10^{-6} \text{ W}$ if the concentration loss started at the current of higher than $132.6 \times 10^{-6} \text{ A}$. Improvement of proton transportation from

anode to cathode chambers such as an adjustment of wastewater flow rate, a modification of influent concentration, etc. should be taken into account to increase P_{max} of BMFCs in our future study.

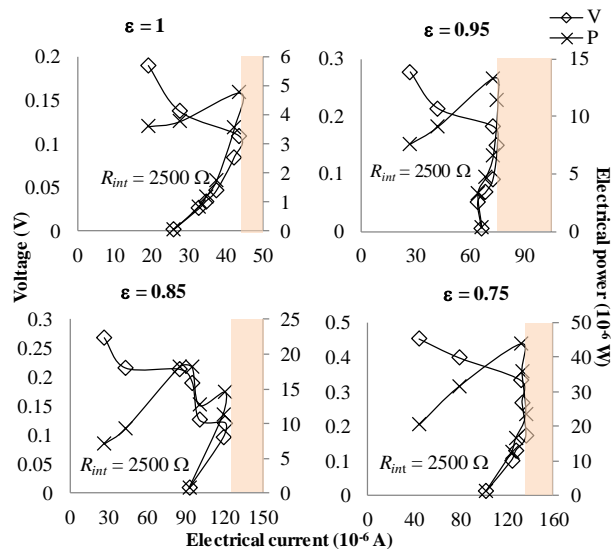


Fig. 5. Results of polarization experiment at the last day of landfill leachate treatment (shade areas were considered to be the concentration loss regions).

3.4 Shear stress and biomass attached to the filter media

Table 1 and Fig. 6 demonstrated τ , m_b , COD removal rate, and P_{max} at the last day of the treatment operation. Good correlation between τ and ϵ as well as high determination coefficients ($R^2=0.954$ to 0.999) of function m_b (τ) and function P_{max} (τ) in Fig. 6 suggested that higher τ resulted from lower ϵ and associated with larger amount of β which caused higher P_{max} . One possible explanation is that microorganisms under adverse growth conditions (i.e., high hydrodynamic shear stress) prefer to migrate toward the more internal layers of the biofilm colonizing all the empty space inside the biofilm [8]. This process probably increases the biomass density biofilm [8] which enhanced the electrogenesis process in anode chambers and thus resulted in the increase of P_{max} . With larger amount of microorganism under high shear stress, biodegradation should enormously occur, thus removal efficiency of COD became high. It was noted that τ ($61.7\text{-}783.9 \text{ }\mu\text{dyn/cm}^2$) values estimated in this research were far from those of Di Iaconi et al. ($5.7\text{-}18.7 \text{ dyn/cm}^2$) [8]. The difference could result from many factors, such as the difference between ϵ in this study (0.75-1.0) and ϵ measured in their study (0.10-0.22) [8], the reactor configuration which was continuous plug flow in this study and sequencing batch biofilm in their study [8], etc. Therefore, direct comparison between τ in this study and τ in the study of Di Iaconi et al. was not bring into further discussion.

Table 1. Parameters observed at each BMFC

Parameters	Bed porosity (ϵ)			
	1	0.95	0.85	0.75
Shear stress (□, $\mu\text{dyn}/\text{cm}^2$)	61.7	152.5	400.4	783.9
Biomass attached to media surface (□, mg/B-MFC)	No media	16.05	34.00	66.02
COD removal rate (mgCOD/L-hr)	970.5	2006.7	2262. 6	3565. 2
P_{\max} (μW)	4.7	13	18	44
HRT (hr)	3.52	3.36	2.98	2.80

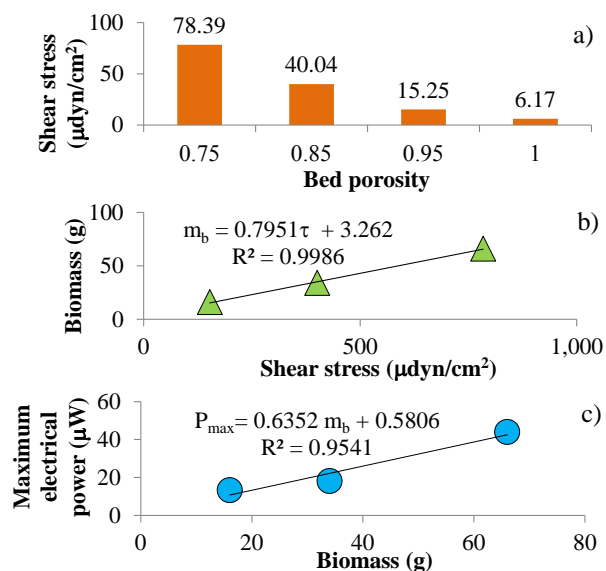


Fig. 6. Relationship between a) media bed porosity and shear stress, b) shear stress and total biomass attached to the filter media, c) total biomass attached to the filter media and maximum electrical power.

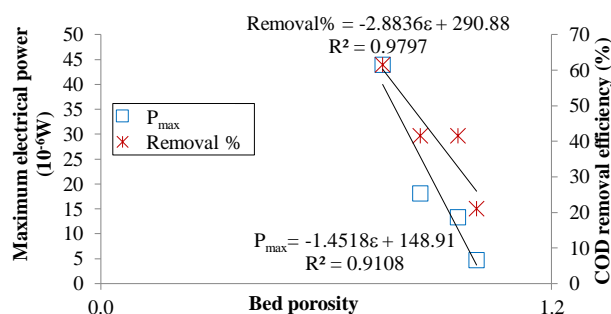


Fig. 7. Roles of media bed porosity in power generating and COD removal.

According to Fig. 7, P_{\max} and COD removal efficiency (Removal %) could be demonstrated as the functions of media bed porosity with remarkable determination

coefficient ($R^2 = 0.91-0.98$). Therefore, to enhance the power generation of BMFCs, the adjustment of media bed porosity which increases the shear stress should be taken into account.

4. CONCLUSIONS

Media bed porosity plays an important role as the shear stress and biomass controller for BMFC performance. High electrical power and COD removal efficiency were achieved at low media bed porosity which produced high shear stress for the scaled-up BMFC. At bed porosity in the range of 0.75 to 1, the BMFC achieved the highest performance at 0.75 bed porosity with 61.6% of COD removal efficiency and 43.96×10^{-6} W of maximum power generation. As the power output of 1-cell BMFC in this research is not sufficient for any electrical devices, these BMFCs are mainly for wastewater treatment. For producing the electricity, further improvement of power output and the application of stacked BMFCs should be taken into account.

5. ACKNOWLEDGEMENTS

This research was supported by Kurita-AIT Research Grant from Kurita Water and Environment Foundation (KWEF) and Doctoral Research Grant from Faculty of Engineering, Mahasarakham University. We are grateful to our colleagues Natchanan Jokloy and Deelters Chankumung for their great assistance in TS and SO_4^{2-} analysis. We also appreciated Asst. Prof. Dr. Chonlatee Photong, Asst. Prof. Dr. Nattawoot Suwanta, and Asst. Prof. Dr. Chontisa Sukkasem for their precious suggestion on our works.

REFERENCES

- [1] Anand Kumar, K.S., Kumar, S., Saket, R.K., and Rajendran, R. 2019. Technological Aspects of Microbial Fuel Cells and Soil Based Green Energy Conversion System. GMSARN International Journal 13 (2019): 159-170.
- [2] Logan, B.E., Hamelers, B., Rozendal, R., Schröder, U., Keller, J., Freguia, S., Aelterman, P., Verstraete, W., Rabaey, K., 2006. Microbial fuel cells: methodology and technology. J. Environ Sci Technol 40: 5181-5192.
- [3] Rahimnejad, M., Bakeri, G., Najafpour, G., Ghasemi, M., Oh, S.E. 2014. A review on the effect of proton exchange membranes in microbial fuel cells. Biofuel Research Journal 1 (2014): 7-15.
- [4] You, S.J., Zhao, Q.L., Jiang, J.Q., Zhang, J.N.. 2006. Treatment of with Simultaneous Electricity Generation in Microbial Fuel Cell under Continuous Operation. Chem Biochem Eng Q 20: 407-412.
- [5] Sonawane, J.M., Ghosh, P.C., 2017. Landfill Leachate: A promising substrate for microbial fuel cells. Int. J. Environ Eng Ecol 11: 418-421.
- [6] Sukkasem, C., Laehlah, S., Hniman, A., O'thong, S., Boonsawang, P., Rarngnarong, A., Nisoa, M., Kirdongmee, P., 2011. Upflow bio-filter circuit (UBFC): Biocatalyst microbial fuel cell (MFC) configuration and application to

- biodiesel wastewater treatment. *J. Bioresour Technol.* 102: 10363-10370.
- [7] Li, H.R., Feng, Y.L., Tang, X.H., Zhang, J.J., Lian, J., 2010. The Factors Affecting Biofilm Formation in the Mediatorless Microbial Fuel Cell. *Chem Biochem Eng Q* 24: 341-346.
- [8] Di Iaconi, C., Ramadori, R., Lopez, A., Passino, R., 2005. Hydraulic Shear Stress Calculation in a Sequencing Batch Biofilm Reactor with Granular Biomass. *J. Environ Sci Technol.* 39: 889-894.
- [9] Pham, H.T., Boon, N., Aelterman, P., Clauwaert, P., Schampelaire, L.D., Oostveldt, P.V., Verbeken, K., Rabaey, K., Verstraete, W., 2008. High shear enrichment improves the performance of the anodophilic microbial consortium in a microbial fuel cell. *J. Microb Biotechnol.* 1: 487-496.
- [10] Halim, A.A., Abidin, N.N.Z., Awang, N., Ithnin, A., Othman, M.S., Wahab, M.I. 2011. Ammonia and COD removal from synthetic leachate using rice husk composite adsorbent. *J. Urban Environ Eng.* 5: 24-31.
- [11] Kamau, J.M., Mbui, D.N., Mwaniki, J.M., Mwaura, F.B., Kamau, G.N., 2017. Microbial Fuel Cells: Influence of external resistors on power, current and power density. *J. Thermodyn Catal.* 8: 182.
- [12] Mashkour, M., Rahimnejad, M. 2010. Effect of various carbon-based cathode electrodes on the performance of microbial fuel cell. *Biofuel Research Journal* 8 (2015): 296-300.
- [13] Izadi P., Rahimnejad M. 2014. Simultaneous electricity generation and sulfide removal via a dual chamber microbial fuel cell. *Biofuel Research Journal* 1 (2014): 34-38.
- [14] Zhang, P.Y., Liu, Z.L., 2010., Experimental study of the microbial fuel cell internal resistance. *J. Power Sources* 195: 8013-8018.